Eur Biophys J (2004) 33: 671–682
DOI 10.1007/s00249-004-0410-7

ARTICLE

Nikolay Korolev · Alexander P. Lyubartsev
Aatto Laaksonen · Lars Nordenskiöld

A molecular dynamics simulation study of polyamine– and sodium–DNA. Interplay between polyamine binding and DNA structure

Received: 18 February 2004 / Revised: 2 April 2004 / Accepted: 5 April 2004 / Published online: 14 May 2004

Abstract Four different molecular dynamics (MD) simulations have been performed for infinitely long ordered DNA molecules with different counterions, namely the two natural polyamines spermidine(3+) (Spd^{3+}) and putrescine(2+) (Put^{2+}), the synthetic polyamine diaminopropane(2+) (DAP^{2+}), and the simple monovalent cation Na^+. All systems comprised a periodical hexagonal cell with three identical DNA decamers, 15 water molecules per nucleotide, and counterions balancing the DNA charge. The simulation setup mimics the DNA state in oriented DNA fibers, previously studied using NMR and other experimental methods. In this paper the interplay between polyamine binding and local DNA structure is analyzed by investigating how and if the minor groove width of DNA depends on the presence and dynamics of the counterions. The results of the MD simulations reveal principal differences in the polyamine–DNA interactions between the natural [spermine(4+), Spd^{3+}, Put^{2+}] and the synthetic (DAP^{2+}) polyamines.

Keywords Cation–DNA interactions · Polyelectrolytes · Putrescine · Spermidine · Spermine

Abbreviations DAP: diaminopropane · DDD: Drew–Dickerson dodecamer · MD: molecular dynamics · Put: putrescine · RDF: radial distribution function · Spd: spermidine · Spm: spermine

N. Korolev · L. Nordenskiöld (✉)
School of Biological Sciences,
Nanyang Technological University,
60 Nanyang Drive, Singapore, 637551
E-mail: larsnor@ntu.edu.sg
Tel.: +65-6136-2856
Fax: +65-6791-3856

A. P. Lyubartsev · A. Laaksonen
Division of Physical Chemistry, Arrhenius Laboratory,
Stockholm University, 106 91 Stockholm, Sweden

Introduction

The delicate interplay between DNA structure, its hydration, and interactions with various ligands, including mobile counterions, has recently become an object of extensive interdisciplinary studies (Chiu et al. 1999; Hud et al. 1999; McFail-Isom et al. 1999; Hamelberg et al. 2000; McConnell and Beveridge 2000; Williams and Maher 2000; Egli 2002) (and references cited therein). Results obtained by experimental (X-ray crystallography, NMR spectroscopy, fluorescence depolarization) and computational methods are in general agreement concerning the structure and dynamics of the DNA double helix and solvent (water) molecules surrounding DNA polymers and oligomers. However, the participation and specific role of the counterions in modulation of the DNA structure and perturbation of the solvation shell around DNA has been much debated in recent literature (Chiu et al. 1999; McFail-Isom et al. 1999; Bonvin 2000; Hamelberg et al. 2000; McConnell and Beveridge 2000; Williams and Maher 2000; Egli 2002). Some workers support the idea of a rapid and sensitive response of the DNA subgroups to the presence of monovalent ions (like Na^+) in the vicinity of electronegative sites of the bases in the grooves and to phosphate groups (McFail-Isom et al. 1999; Hamelberg et al. 2000, 2001, 2002). On the other hand, the opposite opinion does exist which rejects even the possibility for the monovalent cations to be present in the first solvation shell of the DNA, thus making it impossible for these ions to influence the DNA structure (Chiu et al. 1999; Chiu and Dickerson 2000).

The issue of the influence of DNA structure in response to ion and ligand binding is of interest due to the fact that DNA in vivo exists in the form of chromatin, a DNA–protein complex, where the DNA is highly packed and bent. It is proposed that the major force producing bending of the DNA in chromatin could come from an asymmetric neutralization of the DNA

charge on the phosphate groups interacting with the charged amino acids on the surface of the histone octamer of the nucleosome (Manning et al. 1989; Maher 1998). This bending has been confirmed in experiments and simulation with synthetic analogs of DNA oligomers where the phosphate charge has been switched off by chemical modification (Williams and Maher 2000; Kosikov et al. 2002). Furthermore, X-ray diffraction analysis of the nucleosome structure reported narrowing of the DNA minor groove and DNA bending at the sites where Arg^+ residues form stable ionic bonds with the charged oxygen atoms of the DNA phosphate group (Luger et al. 1997; Luger and Richmond 1998).

The naturally occurring tetravalent polyamine spermine (Spm^{4+}) is used in high concentration in the crystallization of DNA (Timsit and Moras 1992). Its role in binding to DNA and in modulation of DNA structure is unclear, since this component mostly escapes detection in the B-DNA crystals (Korolev et al. 2001). Detailed analysis of the most studied DNA oligomer, the Drew–Dickerson dodecamer (DDD), $(dCGCGAATTCGCG)_2$, showed that some narrowing of the minor groove is observed for the crystals grown in the presence of high Spm^{4+} or Mg^{2+} concentrations (Sines et al. 2000). More importantly, however, is that spermine and some other polyamines are present in millimolar concentrations in all eukaryotic cells and play a significant, but not yet clearly resolved, role in biological reactions involving DNA and RNA (Cohen 1998; Igarashi and Kashiwagi 2000). Polyamines and their analogs are also considered as potential anticancer drugs (Thomas and Thomas 2001). Therefore, it is essential to reveal the differences between natural and synthetic polyamines in their interactions with biomolecules and to investigate how ligand (cation) binding can alter (locally and globally) the DNA structure, since it is shown that the polyamines, for example, facilitate a B–Z transition of oligo- and polynucleotides enriched in (GC) dinucleotide steps (Ho and Mooers 1997) or influence equilibrium between A- and B-forms in oriented DNA fibers (van Dam et al. 2002).

This paper describes the final part of a systematic comparative molecular dynamics (MD) computer simulation study of three polyamine–DNA and one Na–DNA systems in a densely packed DNA environment corresponding to oriented fibers or crystals of DNA (Korolev et al. 2003, 2004). The synthetic polyamine diaminopropane(2+) [DAP^{2+}: NH_3^+-$(CH_2)_3$-NH_3^+] and the two natural polyamines putrescine(2+) [Put^{2+}: NH_3^+-$(CH_2)_4$-NH_3^+] and spermidine(3+) [Spd^{3+}: NH_3^+-$(CH_2)_3$-NH_2^+-$(CH_2)_4$-NH_3^+] have been compared under similar conditions (the same DNA sequence, water content, force field parameters, etc.). The systems are composed of a periodical hexagonal cell with three identical DNA decamers, 15 water molecules per nucleotide, and counterions balancing the DNA charges. Collection of trajectories was performed during 6 ns, and for an additional 3 ns for the DAP^{2+}–DNA system showing the slowest dynamics.

In the first paper (Korolev et al. 2003), the main focus was on general binding and diffusion of the polyamines, Na^+, and water in the simulated crystals. The second work (Korolev et al. 2004) described averaged (global and local) DNA structures, and analyzed sequence-specific binding and dynamics of cations and water molecules around the DNA. In all this work, we consistently pay attention to the differences between the natural (Put^{2+}, Spd^{3+}, and Spm^{4+}; Korolev et al. 2001; 2002) and synthetic (DAP^{2+}) polyamines and look for an explanation of why the former ones but not the latter (DAP^{2+}, very similar to Put^{2+}) are the molecules which have been chosen by Nature. An advantage of our simulation work is that the modeled systems have real analogs, the oriented DNA fibers of the corresponding DNA salts, which have been prepared by the wet spinning technique and studied by diffusion- and relaxation-NMR methods (Lindsay et al. 1988; Song et al. 1997; van Dam et al. 2002). The present MD simulations with 15 water molecules per nucleotide correspond to approximately 95% relative humidity (RH) for DNA fibers of the polyamine salts or 85% RH for the Na–DNA fibers. Satisfactory agreement between experimental water and polyamines diffusion data (van Dam et al. 2002) with the results calculated from MD simulation data (Korolev et al. 2003) makes us confident that other results from the all-atomic molecular dynamics calculations give (at least qualitatively) the correct presentation of the ligand– and water–DNA interactions as well as of the DNA structural and dynamic behavior.

In the present work the major focus is on the interplay between local DNA structure and polyamine/Na^+ binding. To address this issue, we discuss mainly the effect on the width of the minor groove of the DNA decamer. Our choice of this particular characteristic of the DNA structure is motivated by the fact that this parameter is most frequently used in other studies discussing the interplay between cation binding and DNA structure (Hamelberg et al. 2000, 2001, 2002). Furthermore, the width of the minor groove shows quite significant variations and dynamics on the time scale of the MD simulations.

Methods and materials

Computational methods

Four different systems with 20 Spd^{3+}, 30 Put^{2+}, 30 DAP^{2+}, and 60 Na^+ counterions were simulated. The number of counterions in each case was chosen to neutralize the negative charge of the phosphate groups of DNA and the systems contained no co-ions. The systems are abbreviated below as DAP, Put, Spd, and Na/15, where "15" stands for the number of water molecules per nucleotide. We will also use the abbreviation PA/15 referring to all polyamine–DNA simulations with 15 H_2O/nucleotide. The results from these four simulations will be compared with data from two previous simula-

tions (Korolev et al. 2001, 2002). The first of these contained Na^+ counterions (Na/20) while the second one contained a 1/1 (in charge ratio) mixture of Na^+ and Spm^{4+} (Spm/Na). The Na/20 and Spm/Na systems both contained 20 H_2O/nucleotide as well as 4 Cl^- co-ions.

MD simulations have been carried out in a hexagonal cell with periodic boundary conditions imposed in the *x*-, *y*-, and *z*-directions. In all simulations the cell contained three parallel ordered B-DNA decamers, 900 water molecules, and counterions. The sequence of all three double helical DNA decamers in the simulation cell was the same, d(5′-ATGCAGTCAG)·d(5′-TGACTGCATC), with the 3′-end of the each strand connected to the periodic image along the *z*-axis. Such a simulation setup corresponds to an infinite array of parallel ordered DNA, thus mimicking DNA in fibers or crystal-like structures. The periodic boundary conditions along the *z*-direction fix the average DNA twist and help to hold the overall B-like DNA form, while leaving a lot of freedom for local DNA motions (Lyubartsev and Laaksonen 1998; Korolev et al. 2001, 2002; Lohikoski et al. 2003).

The CHARMM 22 force field (MacKerell et al. 1995) was used to model both DNA and the polyamine molecules. For DNA we used the CHARMM parameter files directly. For the polyamines (which are not described in the CHARMM topology files) we used similar structures found in the topology files for proteins, taking lysine fragments as prototypes for the amino groups. Thus, we used "CT2" and "HA" atom types for (CH_2) groups, "NH3" and "HC" types for (NH_3^+), and "NP" and "HC" for the middle (NH_2^+) group of Spm. Water was represented by the flexible simple point charge model (Toukan and Rahman 1985), and sodium counterions by the model suggested by Smith and Dang (1994). This combination of force field parameters has previously been used by us for simulation of a full turn DNA fragment in the presence of different monovalent counterions and polyamine molecules and was shown to reproduce stable, B-form-like DNA structures (Lyubartsev and Laaksonen 1998). It should be noted that the DNA periodicity along the *z*-axis fixes the helical twist (10 base pair per turn) and prevents any major bending of DNA or a transition to A-like structures. Although this effect may in principle affect the ion binding, we expect the influence to be small because the imposed periodicity leaves enough freedom for local motions of the DNA structure. Additional details on this and other technical aspects are given in the computational details and supplementary material of our previous work on this system (Korolev et al. 2003). Thus, the present simulation system may be considered to model an array of infinitely long DNA molecules and oriented fibers prepared from high molecular weight DNA. This system is thus somewhat different from the DNA crystal simulations of oligonucleotides in the cell performed by Darden and co-workers (York et al. 1995; Bevan et al. 2000).

The Nosé–Hoover thermostats and barostats (Martyna et al. 1994) were used in all the simulations to keep the temperature at 300 K and the pressure at 1 atm. The pressure was controlled separately in directions parallel and perpendicular to the DNA axes. A double time step algorithm (Tuckerman et al. 1992) with a short time step of 0.2 fs for fast intramolecular vibrations and short-range (within 5 Å cutoff) intermolecular interactions and a long time step of 2 fs for longer range interactions (within a 13 Å cutoff) was implemented. The Ewald method (Allen and Tildesley 1987) was used to treat the electrostatic interactions. The simulation software was the MDynaMix package (Lyubartsev and Laaksonen 2000).

In the beginning of the simulations, the polyamine molecules were positioned between the DNA molecules at equal distance from each DNA, with water molecules filling the remaining space. A 100 ps run, at constant volume and fixed DNA and polyamine atom coordinates, was initially performed, to allow water molecules to form hydration shells around DNA and the ions. After that, all atoms were released, and the constant-pressure molecular dynamics algorithm started. An additional 200–300 ps run was carried out to allow all atoms to equilibrate, and then a 6 ns production run was performed, during which all distribution functions and statistical averages were calculated. For the DAP system, an additional 3 ns of trajectories were collected (total simulation time for the DAP system was 9.38 ns). For the Na/15 system, an initial configuration was generated from a snapshot of the Na/20 system by randomly removing Cl^- and excess of Na^+ ions and water molecules following the equilibrating procedure applied for the PA/15 systems. After a constant volume equilibration of the system for 100 ps, a constant pressure and temperature MD simulation run was performed with the trajectories collected from 0.3 to 6.4 ns.

The groove width was calculated by program Curves 5.2 (Stofer and Lavery 1994) using the separation between sugar ring oxygen atoms (O4*) as a basis for calculation of the groove width. Therefore, the O1P–O1P radial distribution functions (RDFs) between the closest O1P atoms of the opposite DNA strands (used below in analysis of time-averaged correlations between ion binding and the minor groove width) are *not* equal (though proportional) to the groove width shown in figures analyzing MD snapshots.

Results and discussion

Below we use three different approaches to describe the interplay between DNA structure and ligand binding. First, the width of the DNA minor groove is investigated as a function of DNA sequence for the DNA structure averaged over three decamers and 6 ns of the MD simulations (except for the DAP system where data were collected for 9.38 ns as well). The averaged data are complemented by the sequence dependence of the minor

groove width taken for snapshots at different moments during the simulations. By analyzing the snapshots we investigate if binding of the polyamines and Na^+ correlates with the regions of narrowing of the minor groove.

Secondly, we analyze the dynamics of the polyamine binding at selected locations of the DNA sequence and the dynamic effect on the groove width. The comparison of the data collected for the different systems reveals similarities and differences in interaction of the polyamines with DNA and shows that the polyamines DAP^{2+} and Put^{2+} have different abilities to modulate DNA structure.

Third, we collect and average statistics of the O1P–O1P distance between the phosphate groups across the minor groove and study the correlation of this distance with the presence of cations (amino group of the polyamines or Na^+). This analysis also reveals significant differences between the ligands in modulation of the DNA structure.

Dependence of the minor groove width on the DNA sequence and counterion nature

In Figures 1, 2, 3, 4 the minor groove width along the sequence of the DNA decamer is shown for the DAP, Put, Spd, and Na/15 systems, respectively. For the PA/15 systems (Figs. 1, 2, 3) the central graph in each figure displays the variation of the minor groove width with sequence, averaged over all three decamers and during the simulation. In addition, this width is displayed for selected individual decamers at two instantaneous moments of the MD run: in the middle (at about 3 ns, denoted Mid) and at the end (at about 6.5 ns, denoted End). Furthermore, for the DAP system (Fig. 1) a snapshot taken at the end of an extended simulation is analyzed ($t = 9.38$ ns; denoted Ext). Around the central graph, snapshots taken at the same moment as the instantaneous sequence dependence of the groove width illustrate the position of the polyamines around the sites of particular interest.

DAP is capable of pronounced narrowing of the minor groove through direct binding to the phosphate groups across the groove

A very interesting feature of the DAP system seen in the graph and in the snapshots of Fig. 1 is a pronounced narrowing of the minor groove near the G3 and A5 bases, observed for one of the three decamers. For this decamer, the sequence dependence of the groove width at instantaneous moments of time is displayed. Direct coordination of the DAP^{2+} amino groups to the phosphate groups at these positions (seen from the snapshots) leaves no doubt that the minor groove narrowing at these sites is provoked by the polyamine coordination to the O1P atoms across the groove. At the G3 site

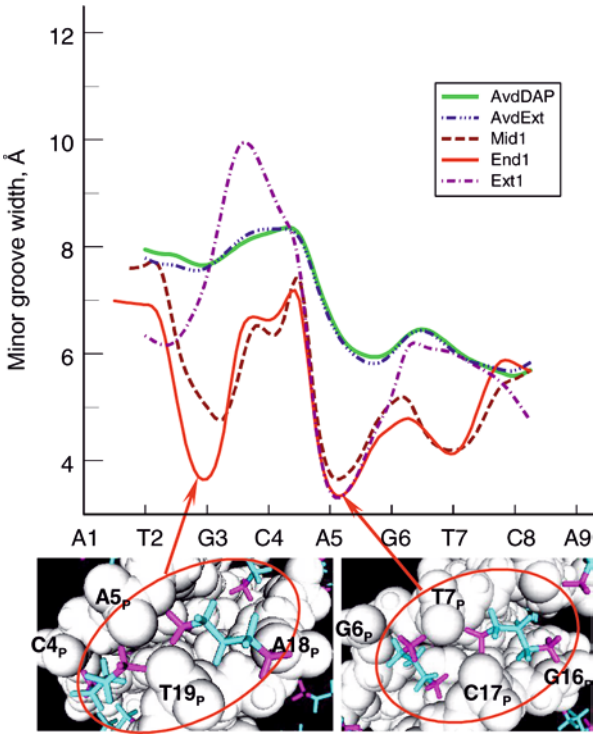

Fig. 1 The change of the minor groove width along the DNA decamer and snapshots showing positions of the DAP^{2+} molecules around DNA. *Green* and *blue lines* show the groove width of the decamer obtained from averaging over three DNA molecules respectively after 6.3 (*solid line*) and 9.38 ns (*dotted line*). The other lines are the instantaneous width for the first DNA molecules in the simulation cell, calculated from the decamer structure at the middle (*red dashed line*; $t = 3.9$ ns), end (*bright red solid line*, $t = 6.3$ ns), and after an extended simulation (*magenta dot-dashed line*; $t = 9.38$ ns). In the cartoons, snapshots of the DNA structure illustrate the positions of DAP^{2+} (*sticks*; amino and methylene groups are respectively in *magenta* and *cyan*) for the G3 and A5 base regions of the minor groove. *Arrows* show the corresponding site positions in the DNA double helix displayed in the cartoons

(snapshot in the bottom left side of Fig. 1), a remarkable concerted action of the two DAP^{2+} molecules coordinated to the two O1P atoms of the opposite DNA strands is observed. Thus, attachment of the two DAP^{2+} molecules to the O1P atoms forms a "stitch", giving a very short distance between the phosphates. The entire structure is additionally stabilized by binding of the second amino group of each of the DAP^{2+} molecules to the neighboring O1P atoms along opposite strands of the DNA double helix. The high symmetry of the observed structure, and its exceptional stability during the time between the midpoint of the simulation until the end of the "regular" 6 ns simulation, led us to extend the simulation of the DAP system for an additional 3 ns to a total simulation time 9.38 ns. After 7 ns it was observed that one of the two DAP^{2+} molecules dissociates from the site, and the other DAP^{2+} keeps only one hydrogen bond to O1P. Dissociation of the DAP^{2+}–DNA contacts leads to an increase in the minor groove width near the G3 site at the end of the extended MD run (red dotted curve in Fig. 1). The other regions

of the minor groove show slower dynamics, although some changes in the groove were observed for each of the three DNA decamers in the simulation cell. Interestingly, the dependence of the minor groove width calculated for the averaged DNA structure after 6.3 and 9.38 ns of the MD simulations does not show any noticeable variation, despite changes in the groove geometry of the individual DNA decamers in the simulation cell.

Similar to the G3 site, two DAP^{2+} ligands participate in the narrowing of the minor groove at the A5 position (bottom right hand cartoon in Fig. 1). However, at this site, the groove narrowing and DAP^{2+} binding have a somewhat different structure since only one of the DAP^{2+} molecules binds to the DNA in a way similar to the symmetrical binding at the G3 site. The second DAP^{2+} molecule forms a hydrogen bond with only one of two O1P atoms at the groove narrowing situated beneath the phosphate groups, inside the minor groove. The DAP^{2+} binding at the A5 site displays stability during the extended simulation.

A narrowing of the narrow minor groove at the G6 base of the second DNA decamer is also observed (data not shown). Here (as in the previous cases), two amino groups from two DAP^{2+} molecules interact with both O1P atoms of the opposite DNA strands, closing "the lips" of the minor groove.

Snapshots for the second and third DNA molecules in the simulation cell in the same region around the G3 site exhibit relatively wide minor groove widths (data not shown). Here, the widening of the minor groove is not due to the absence of polyamine molecules in this region since several DAP^{2+} molecules can be observed. However, their binding does not result in the narrowing of the groove. Obviously, not only the presence but also the geometry and the "concerted" action of the ligands are essential for modulation of the DNA structure.

Putrescine binding in and around the minor groove

Similar to the DAP system, two sites with the narrow minor groove are seen at the site of the G3 and A5 bases of the first DNA oligomer in the simulation cell (Fig. 2, red curves). However, the role of polyamine binding for modulation of groove geometry is less straightforward compared to the DAP system. At the G3 site of the first decamer of the DAP system, narrowing of the groove is clearly caused by direct interaction with two DAP^{2+} molecules (Fig. 1). In the Put system (Fig. 2), only one polyamine molecule is present near the G3 site during a prolonged period of time (the second Put molecule seen in the bottom-left cartoon in Fig. 2 stays in the vicinity of the site for a very short time). Additionally, near the G3 site, the structure of Put^{2+} binding to DNA is slightly different. A more detailed analysis of the Put^{2+} binding at the G3 site of the first decamer will be presented below.

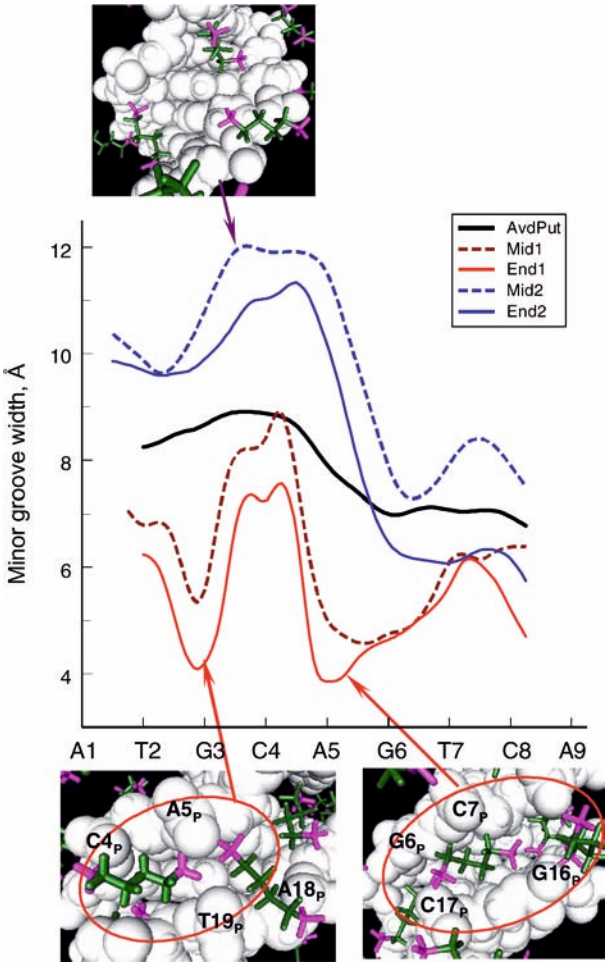

Fig. 2 The change of the minor groove width along the DNA decamer and snapshots showing positions of the Put^{2+} molecules around DNA. In the graph, the *black solid line* shows the minor groove width of the averaged DNA structure; the *thin lines* display instantaneous profiles of the DNA minor groove taken respectively for the first (*red*) and second (*blue*) DNA molecules in the middle (*dashed lines*; $t = 2.8$ ns) and at the end of the simulation (*solid curves*; $t = 6.4$ ns). Snapshots taken at $t = 2.8$ (a cartoon at the *top*) for the second DNA molecule and at $t = 6.4$ ns for the first DNA (two snapshots at the *bottom*). Methylene groups of Put^{2+} are shown in *dark green*

Near the A5 base, the narrowing of the groove is not caused by specific binding of the amino group but by a high presence of polyamines, with up to four Put^{2+} molecules seen in the vicinity of the site (bottom-right cartoon in Fig. 2). The phosphate groups of the opposite DNA strands are not located against each other, but are arranged like a "zipper". Molecules of Put^{2+} lay inside and outside the minor groove and interact with various polar groups of the sugar-phosphate.

The Put system shows higher flexibility with respect to changes in the minor groove width than in the DAP system. In the Put system, the width of the minor groove fluctuates more noticeably and substantial changes in the groove width were observed at several positions during the 6 ns MD simulation.

In the top cartoon of Fig. 2, a snapshot shows the Put^{2+} distribution around a wide region of the minor groove near the G3-C4-A5 bases of the second DNA decamer. One Put^{2+} molecule is located here but it does not bridge between the DNA strands.

Influence of Spd^{3+} on the minor groove width

For the Spd system, an analysis of the minor groove width and polyamine binding is shown in Fig. 3. Narrowing of the minor groove is observed near the sites of the G3 (first decamer, red curve) and T7 (third decamer, blue curve) bases. It is caused by coordination with Spd^{3+} in a way similar to that observed for the DAP and Put systems, i.e. the terminal amino group of Spd^{3+} forms two hydrogen bonds with the O1P atoms from the opposite DNA strands. This is illustrated in the top and in the two bottom cartoons of Fig. 3. These two bottom snapshots illustrate the common groove narrowing in all PA/15 systems caused by alignment of the polyamine molecule along the minor groove in parallel with phosphate groups, which allows formation of hydrogen bonds from one amino group to the two O1P atoms of the opposite strands.

Comparison of three PA/15 systems demonstrates that the polyamine binding and groove narrowing is far less frequent in the Spd system. For this polyamine, the minor groove exhibits more flexibility than in the Put and especially in the DAP systems.

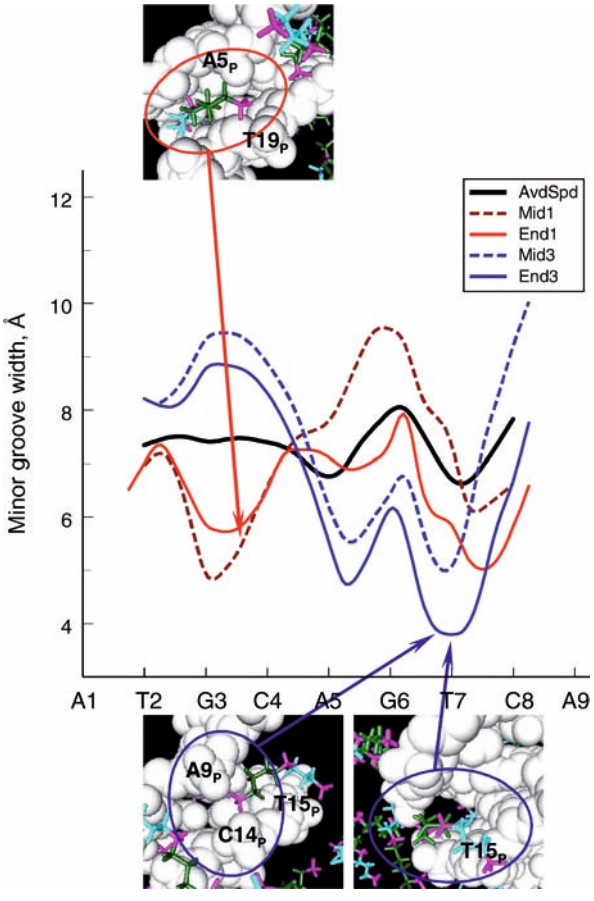

Fig. 3 The change of the minor groove width along the DNA decamer and snapshots showing positions of the Spd^{3+} molecules around DNA. The picture is built using the scheme similar to the one used in Figs. 1 and 2 (except for features listed below). Snapshots were taken at $t = 3.4$ and 6.6 ns. *Blue curves* show the minor groove profile of the third DNA molecule in the simulation cell (not the second DNA as for the Put system analyzed in Fig. 2). The three, $(CH_2)_3$, and four, $(CH_2)_4$, methylene moieties of Spd^{3+} are shown in *cyan* and *dark green*, respectively. In the *bottom* cartoons, the narrowing of the minor groove near the T7 base site is shown as a front view of the minor groove (*left*) and as a view along the minor groove from the top of the decamer (*right*)

Minor groove width in the Na/15 system

Figure 4 shows the change of the minor groove width along the DNA decamer obtained for the Na/15 system. To highlight the differences, the same scale for the ordinate in the graphs of Figs. 1, 2, 3, 4 is used. One can see that Na–DNA (both the averaged structure and each decamer in the simulation cell) generally shows a wider minor groove with significantly less fluctuations in width between the different DNA molecules. At the same time, in the Na/15 system the minor groove profile changes more dynamically with time, displaying much more freedom in movement of the sugar-phosphate backbone in the presence of Na^+ ions compared with polyamine–DNA.

A common feature of the minor groove profiles of the DNA decamers (except the one for the third decamer at $t = 2.9$ ns) is a narrowing of the groove at the A1T2/A18T19 site, which is related to the propeller twist of the T2 and T19 bases, merging two thymine hydration sites ($T2_{O2}$ and $T19_{O2}$) into one, and with the binding of Na^+

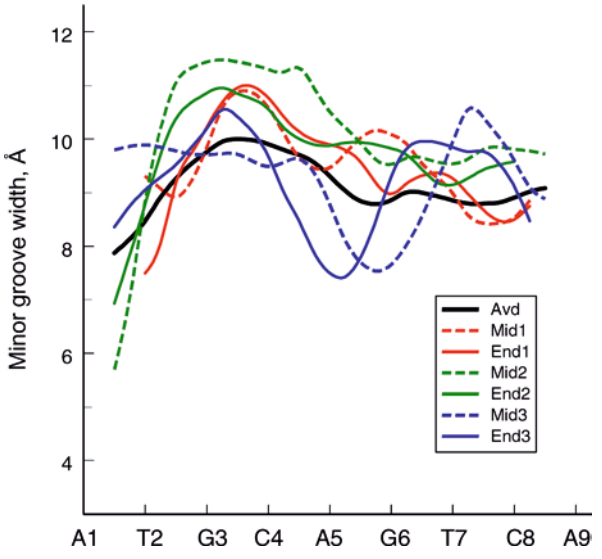

Fig. 4 The dependence of the DNA minor groove width in the Na/15 system determined for the averaged DNA structure (*thick black curve*) and from snapshot structures of each of the three DNA decamers in the simulation cell taken at $t = 2.9$ and 6.7 ns (*dashed and solid lines*, respectively)

at this site. The polyamine binding and corresponding change in the groove width at this region is smaller than for the Na/15 system (analysed in our previous work: Korolev et al. 2004). Important differences exists between the sites of the narrow minor groove in the PA/15 systems and in the A1T2/A18T19 region of the Na/15 system. Thus, for polyamine–DNA, the cause of the narrowing is the presence of a ligand near the lips of the groove and their binding to the O1P atoms, whereas in the Na/15 system [and in the well-studied $(AATT)_2$ region of the DDD decamer (Drew and Dickerson 1981)] the most probable cause of the narrowing is changes at the bottom of the groove: in the local structure of the bases and merging of the hydration T_{O2} (and A_{N3} in DDD) sites. It is still debatable if the cations contribute to this phenomenon (Shui et al. 1998; Chiu et al. 1999; Bonvin 2000; McConnell and Beveridge 2000). In a recent MD simulation study, Williams and co-workers (Hamelberg et al. 2001) detected correlation of the minor groove width at the $(AATT)_2$ region with the presence of Na^+ near the lips of the minor groove. It is unclear, however, how their observation correlates with the X-ray crystallography results from the same group advocating dynamic exchange between water and Na^+ at the T_{O2}/T_{O2} hydration site and the idea that just this effect is responsible for the narrow groove in the middle of the DDD (Shui et al. 1998; Howerton et al. 2001). Our analysis of ion–ion correlations (Korolev et al. 2003) near the two binding sites predicts that the simultaneous presence of *different* ions does not take place if the distance between the binding sites is less than 7–8 Å. That means that in the DDD molecule, only one (maximum two) cations can reside at any moment of time in the $(AATT)_2$ region. Therefore, co-existence of multiple cation binding sites with the hydration sites does not mean that they can be occupied by several ions simultaneously.

Dynamics of polyamine binding to DNA at the sites of the minor groove narrowing

Binding of DAP^{2+} near the sites of the minor groove narrowing

Snapshots taken from the MD trajectories of DAP system reveal a remarkably stable presence of two DAP^{2+} molecules at each of the two sites of the minor groove in front of the G3 and A5 bases of the first DNA decamer (Fig. 1, red curves in the graph, two snapshots at the bottom). DAP^{2+} is the most "sticky" ligand among the polyamines studied in our laboratory experimentally (van Dam et al. 2002) and in silico (Korolev et al. 2001, 2002, 2003, 2004). For this reason, we extended this simulation for an additional 3 ns. Below we present a more detailed analysis of the DAP^{2+} binding near these G3 sites (Fig. 5). We have chosen several atom–atom distances which help to reveal the dynamics of the connection between the DNA structure and DAP^{2+} binding. The time dependence of these interatomic distances during the course of the simulation is displayed in Fig. 5.

Both at the G3 and at the A5 sites, two DAP^{2+} molecules cause narrowing of the groove by binding to the opposite phosphate groups (G3 site: $A5_P$ and $T19_P$; A5 site: $T7_P$ and $C17_P$). In Fig. 5, trajectories which characterize the binding of each of the two DAP^{2+} molecules are shown separately for the molecules sitting respectively above (three panels at the top) and below (three panels at the bottom) the site of the groove narrowing. In the central panel of Fig. 5 the bright red curve shows the time dependence of the minor groove width, characterized by the O1P–O1P distance at the narrow site.

Near the G3 base (Fig. 5; see also bottom left snapshot in Fig. 1) a very narrow minor groove (O1P–O1P distance is 4.5 Å or less) is observed at about 1.2–2.4 ns and 4–7 ns (bright red curve in central panel of Fig. 5). One of the two DAP^{2+} molecules is attached to the C4 and T19 phosphate groups almost all the time from 1 to 7.2 ns of the simulation (blue and green curves in two bottom panels of Fig. 5). The binding of the amino group from the other DAP^{2+} molecule to the same O1P atoms is more dynamic (blue and green curves; second and third panels from the top of Fig. 5). The closest O1P–O1P distance (3 Å) is observed when two amino groups of different DAP^{2+} molecules coordinate directly to the $A5_{O1P}$ and $T19_{O1P}$ atoms from the opposite DNA strands at the "lips" of the minor groove. The unique geometry of this coordination of two O1P atoms with two amino groups of the different DAP^{2+} molecules is not observed for any other polyamine we have studied. At about 7.2 ns, one of the DAP^{2+} molecules dissociates from the C4-A5 site (two bottom curves in Fig. 5). This event is accompanied by opening of the minor groove near the G3 base (bright red curve in the middle of Fig. 5).

Binding of DAP^{2+} *along* each of the strands freezes the O1P–O1P distance at about 6 Å (grey and black curves in Fig. 5). Similar distances at other positions and for the other polyamines show quite a broad variations during the simulation (data not shown). Apparently, the short (compared with the other polyamines) length of DAP^{2+} matches the O1P–O1P separation in the DNA polynucleotide chain, allowing this polyamine strong binding along the DNA strand.

For the A5 position of the first decamer, the groove narrowing occurs during the second half of the MD simulation. After 5 ns the distance between $T7_{O1P}$ and $C17_{O1P}$ drops from 5–7 Å to about 4 Å (data not shown). Binding of one of the two DAP^{2+} molecules at the A5 site is quite similar to that seen for DAP^{2+} at the G3 site.

The DAP^{2+} binding to the G3 and A5 bases demonstrates that stable and direct coordination of the DAP^{2+} amino groups to the DNA phosphates not only distorts the DNA structure, but also changes both the sign and spatial distribution of the electrostatic field at

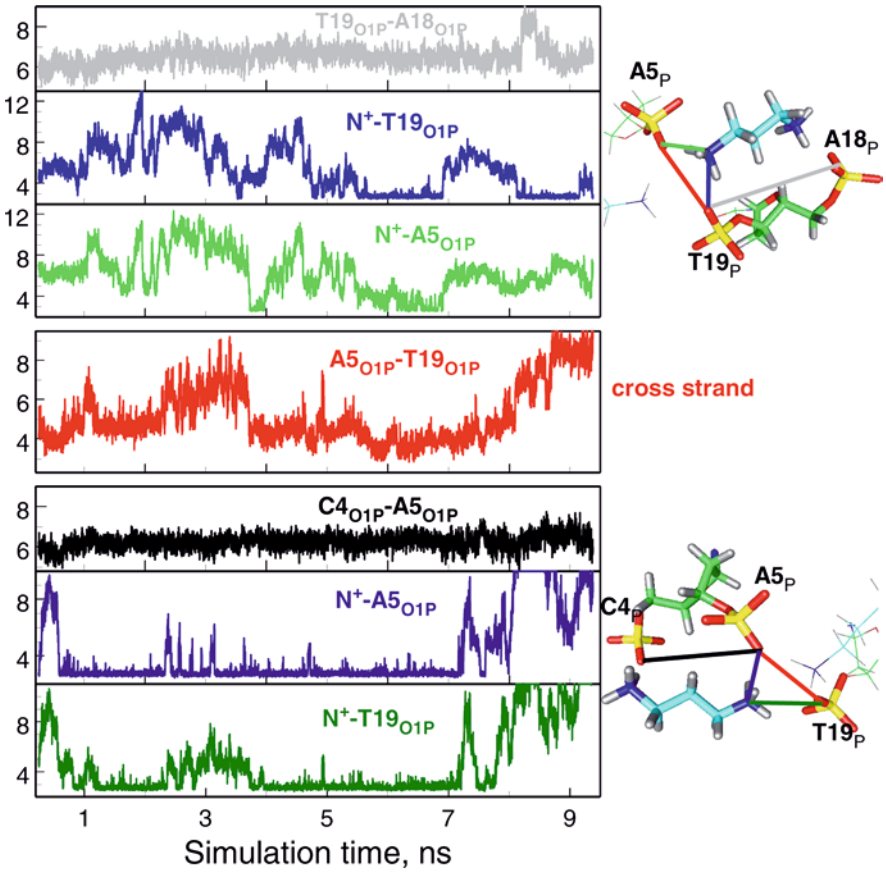

Fig. 5 Interplay between dynamics of DAP binding and local DNA structure near the site of the G3 base (corresponding to Fig. 1, *left-bottom snapshot*). Dynamics of atom–atom distances between selected atoms of DNA and atoms of the DAP^{2+} molecule located at the top of the G3 site and interacting with the A18-T19 nucleotides is displayed in the *three top panels*. The *fourth panel* from the top (*bright-red curve*) shows the time dependence of the O1P–O1P cross-strand distance at the site of narrowing. The *three bottom panels* describe dynamics of atom–atom distances for binding of the second DAP^{2+} molecule (located below the G3 site and interacting with C4-A5 nucleotides). The color scheme is explained in the *right-hand cartoons* showing the two snapshots centered on the DAP^{2+} molecules under analysis; in each panel, the analyzed atom–atom distance is marked

the binding sites. For the other polyamines we have studied (the natural Put^{2+}, Spd^{3+}, and Spm^{4+}), cases of such strong polyamine binding and influence on the DNA structure are observed to a much lesser extent only for Put^{2+} (see below). If DAP^{2+} were present in living cells, the alterations of the DNA structure and local charge distribution caused by the DAP^{2+} coordination could disrupt specific and nonspecific DNA binding, recognition by ligands, or could create "a stumbling block" for the operation of RNA/DNA polymerases, chromatin remodeling complexes, or regulatory proteins searching for their recognition sequences.

Put^{2+} and Spd^{3+} binding and minor groove narrowing at the selected sites

The dynamic interplay between polyamine binding and the minor groove width is shown for the sites of the minor groove narrowing in the Put (Fig. 6a) and in Spd (Fig. 6b) systems. For the Put system, the groove narrowing is observed at the G3 site of the first decamer. Although the snapshot shown in the bottom-left cartoon of Fig. 2 gives an impression that two Put^{2+} molecules are bound at this site, analysis of the trajectories reveals that the second Put^{2+} molecule stays there for very short time only (data not shown). Unlike the DAP system, in the Put system the $A5_{O1P}$–$T19_{O1P}$ distance never drops below 4 Å. Between 1 and 2.8 ns, the Put^{2+} molecule (which is responsible for the later groove narrowing) does not bind to any of the O1P atoms in the vicinity of the G3 site. Then the Put^{2+} molecule comes closer to the C4-A5 nucleotides and at about 3 ns binds to $C4_{O1P}$ (magenta curve, second panel from the top). Simultaneously, stabilization of the O1P–O1P distance along the DNA strand between the C4 and A5 bases occurs (grey curve, top panel in Fig. 6a). At about 4 ns, a bond is formed between the other amino group of Put^{2+} and $A5_{O1P}$ (blue curve, third panel from the top), accompanied by narrowing of the minor groove (red curve). The Put^{2+} molecule is observed to make bridges between two opposite DNA strands (direct hydrogen bonds with $C4_{O1P}$ and $T19_{O1P}$ atoms *across* the groove; magenta and blue curves of Fig. 6a). This structure of the polyamine–DNA complex is different from DAP^{2+} binding at the G3 site, where both DAP^{2+} molecules prefer to make hydrogen bonds with neighboring phosphates *along* the DNA strand. In general, Put^{2+} binding to the phosphate groups is more "loose" and produces a less destructive influence on the minor groove width and other parameters of the B-DNA double helix. (Korolev et al. 2004)

For the Spd system, a similar analysis is presented in Fig. 6b, where minor groove narrowing is observed near the T7 base of the third DNA molecule (also shown in two bottom snapshots of Fig. 3). Somewhat unexpectedly, the narrowing of the groove near the T7 site is modulated by the four-methylene part of Spd^{3+} (where the separation between amino groups is the same as in

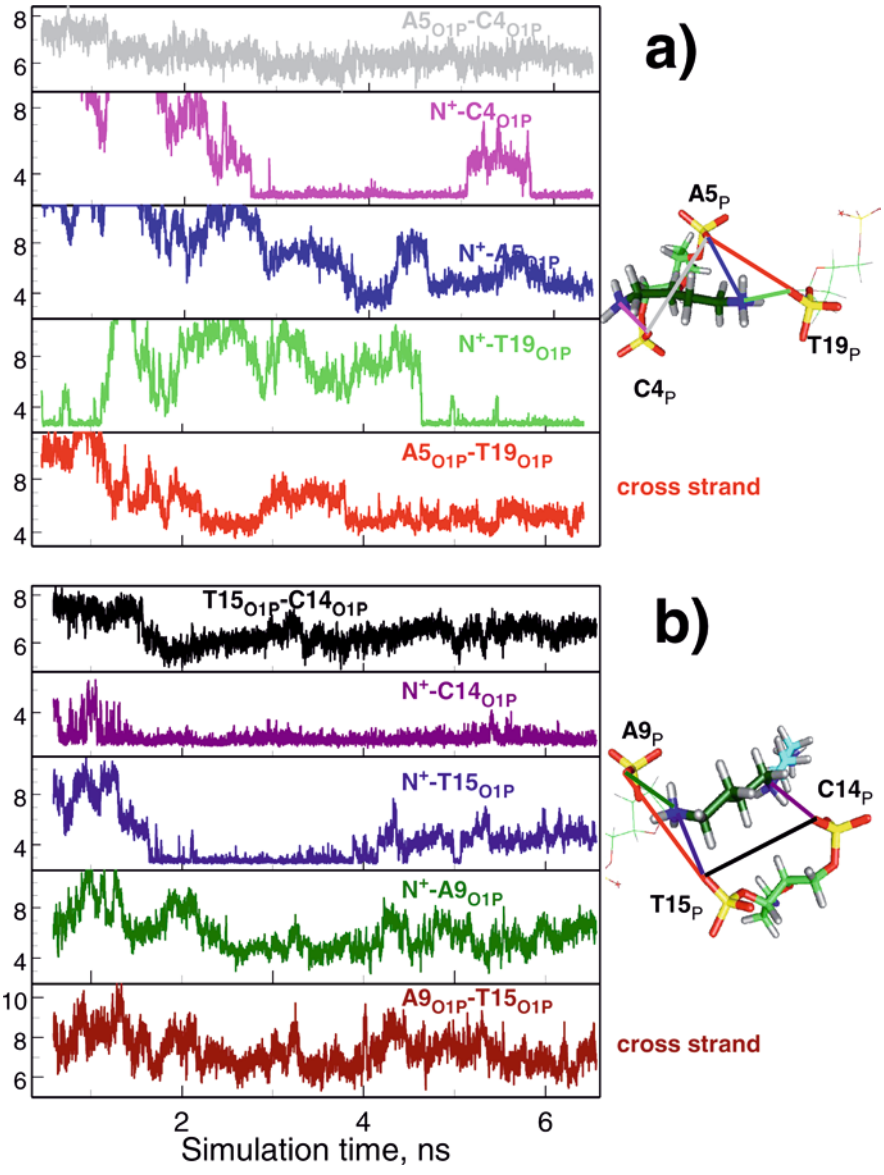

Fig. 6a, b Interplay between the dynamics of Put and Spd binding with local DNA structure. The figure was drawn using the same scheme as in Fig. 5. (**a**) Put system: the site of the groove narrowing near the G3 base (also shown in Fig. 2, bottom-right snapshot). (**b**) Spd system: the site of the groove narrowing near the T7 base (also shown in Fig. 3, two cartoons at the bottom snapshot)

Put^{2+}) and not by the more "sticky", DAP-like three-methylene moiety. The O1P–O1P distance between opposite phosphate groups near the T7 site ($A9_{O1P}$–$T15_{O1P}$ distance, red curve in Fig. 7b) drops to 4–5 Å only rarely (this moment is shown in the cartoons at the bottom of Fig. 3) and remains mostly in the region of 6–8 Å. As has been observed for the DAP and Put systems, an important factor in the minor groove narrowing mediated by the polyamine binding is an additional coordination to one of the neighboring phosphate groups. In the Spd system the central (N5) amino group maintains a direct hydrogen bond with $C14_{O1P}$ through most of the simulation (magenta curve, Fig. 6b). Unlike Put^{2+} (which connects opposite DNA strands, see above), the terminal amino group of Spd^{3+} (N10) is mainly along one of the DNA strands (interacts with $T15_{O1P}$, while the central N5 atom binds to $C14_{O1P}$; blue and magenta curves respectively, Fig. 6b). This mode of binding does not seem to fit the length of the stretched four-methylene chain and leads to bending of the polyamine and may in turn cause an increase of the groove width. In the Spd system, the DNA structure generally shows more flexibility than in the DAP system.

Statistically averaged correlations between O1P–O1P separation and the polyamine presence in the vicinity of phosphate groups

So far, in the description of our MD simulation results we considered selected polyamine molecules and specific locations in the DNA molecule. Most experimental techniques, however, do not allow observation of the binding and dynamics at this level of resolution; rather, time- and system-averaged characteristics can be obtained. Below we will present time and system averages which describe the "general" influence of different ligands on the width of the minor groove the (O1P–O1P

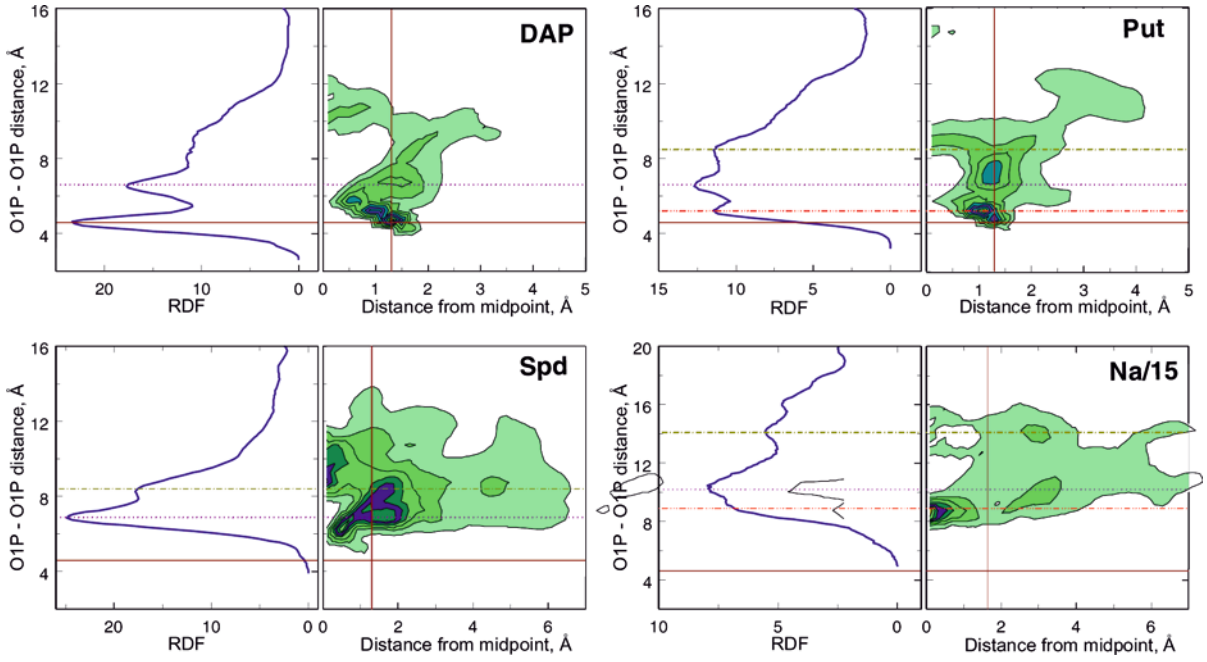

Fig. 7 Correlation between the averaged O1P–O1P distance and the cation presence between and close to the O1P atoms across the minor groove. Each of the four panels consists of two graphs, calculated from the MD simulation trajectories collected respectively for the DAP, Put, Spd, and Na/15 systems. The *left-hand graph* in each panel displays the total RDFs between all pairs of two O1P that belong to opposite DNA strands and are closest to each other across the minor groove. For B-DNA these are from the $(i+3)$ base pair. The *ordinate* is the O1P–O1P distance; the *abscissa* shows the relative density of the atom–atom distribution. All ten O1P–O1P pairs have been averaged, which calculated as a sum of all. The *right-hand graph* of each panel presents a "3-D RDF", where the normalized density of an atom of the mobile ligand (N^+ atom of the polyamine or metal ion) is determined as a function of the O1P–O1P separation (*ordinate*) and the distance of the charged group to the middle point connecting the O1P atoms (*abscissa*). The coordinate system we have chosen to determine "the 3-D RDF" is similar to that proposed by Hamelberg et al. (2001). The *red vertical* and *horizontal* bars represent the "ideal" values of these variables that would be expected for a free cation complex with two O1P groups (see the text for details)

distance across the groove). To make this estimation we have used an approach similar to the one described by Hamelberg et al. (2001). We consider the middle point of the line connecting two O1P atoms across the groove and analyze the distribution of cations (polyamine nitrogen atoms and Na^+) relative to this point and its dependence on the O1P–O1P distance. In this way, "3-D RDFs" were calculated, where the cation density is presented as a function of two distances: the O1P–O1P separation and the cation–middle point of the O1P–O1P distance.

3-D RDFs are presented in the right panels of each of the four sections of Fig. 7, together with RDFs (left panels) summed over all ten O1P–O1P pairs in the decamer solid line. To highlight the difference in the ability of various cations to modulate the minor groove width, the solid red bars show the distance between the O1P atoms (horizontal bar) and the distance from the nitrogen atom to the middle of the line connecting these atoms (vertical bars), which corresponds to an "ideal" coordination of the cation group to the two (arbitrary) oxygen atoms. These "ideal" distances have been determined by assigning a 1.4 Å hydrogen bond length, a 60° H–N...O angle for the NH_3^+–oxygen coordination, a 2.3 Å Na^+...O distance, and a 90° O...Na^+...O angle for the Na^+ binding. Appearance of maxima both in the O1P–O1P RDF (on the horizontal bar) and in the 3D-RDF (at the crossing points of the bars) means that the ligand is able to coordinate with the O1P atoms of DNA according to the geometry which is ideal for the ligand (even if this binding influences the regular structure of B-DNA). One can see that among the cations we have studied, only DAP^{2+} (and Put^{2+} to a lesser extent) possesses such an ability. More close comparison of the RDFs of the DAP and Put systems reveals that in the DAP system there are five specific O1P–O1P pairs showing a maximum near the horizontal bar, while in the Put system the corresponding peak is observed only for two O1P–O1P pairs (data not shown). In the Put system, the intensity of the second (not the first as in the DAP system) maximum in the O1P–O1P RDFs is the highest and correlates with the presence of the amino groups roughly in the second solvation layer of the phosphate group and shifted from the midpoint of the O1P–O1P line by about 1.3 Å. In the Spd system (bottom left panel in Fig. 7) the amino groups do not show the ability of bringing together the two O1P atoms of the opposite DNA strands. The bar crossing the 3D-RDF (right) panel shows no intensity and the most populated O1P–O1P distance (left panel) is about 7 Å, which is close to the distance in the regular structure of B-DNA and correlates with coordination of the polyamine in the second hydration shell of the phosphate group.

In the Na/15 system (bottom right panel in Fig. 7) the maxima of the O1P–O1P RDFs are shifted to 8–12 Å;

sodium ions are mainly distributed around the O1P–O1P midpoint. This position of Na^+ corresponds to Na^+ coordination in the second solvation shell of the phosphate group. Thus, the ability of the sodium ion to modulate the DNA structure is substantially weaker than that of the polyamines. The distance between the O1P atoms varies in a broad range, and the intensities of the total and individual maxima of the O1P–O1P RDFs are rather low, which demonstrates the flexible dynamic behavior of the phosphates in B-DNA, even in the system where DNA movement should be substantially repressed due to the low hydration, strong packaging forces, and periodic restrictions along the B-DNA helical axis.

We performed similar analyses for the other systems studied in our laboratory earlier, i.e. the mixed Spm/Na system and the Na/20 system (Korolev et al. 2001, 2002), both with 20 water molecules per nucleotide (data not shown). Comparison of all data obtained shows that DAP^{2+} (and Put^{2+} to a much lesser extent) has a unique ability to coordinate simultaneously to the two oxygen atoms of a phosphate group and in this way significantly disturb the DNA structure. The polyamines Spd^{3+} and Spm^{4+}, which are naturally occurring in eukaryotic cells, do not have this potency despite their high positive charge.

Conclusion

In contrast to the MD simulation data reported by Williams and co-workers (Hamelberg et al. 2000; 2001) advocating rapid and sensitive response of the DNA phosphate group (accompanied by the appropriate change in the minor groove width) due to the movements of Na^+, our data argue against a direct and straightforward modulation of the local DNA structure by this monovalent cation (see also our previous work: Korolev et al. 2002). This sustains the results of McConnell and Beveridge (2000) in support of an indirect and complex response of the DNA structure on movements of the cations. The systems we have studied (packed environment, low water content, periodical restriction along the *z*-axis) are relevant to real experimental systems under investigation in oriented fibers and crystals of ordered DNA.

The low capacity of the monovalent cations to modulate the DNA structure becomes more pronounced when this is compared with the effects of the polyamines (especially with DAP^{2+}) in this respect. We argue that the decisive factor that facilitates the ability of the ligand to modulate the local DNA structure is the possibility for the ligand to statically reside in the vicinity of DNA. This is clear from the correlation in formation of the O1P...H_3N^+ ionic pair between DAP^{2+} and the phosphate group next to the site of the groove narrowing as well as coordination of the second DAP^{2+} molecule to the O1P atoms at the site of the groove narrowing (Fig. 5). This property of DAP^{2+} makes this ligand somewhat similar to the Arg^+ residues of the histones which modulate narrowing of the minor groove by formation of ionic bonds with the phosphate groups of DNA in the nucleosome (Luger et al. 1997; Luger and Richmond 1998). It would be interesting in this respect to study if the binding of the guanidinium group of arginine could change the DNA structure by itself or if it acts in concert with static fixation of this charged ligand near the position of binding. Notably, our results reveal that the natural eukaryotic polyamines, Spd^{3+} and Spm^{4+}, do not have a similar (to the synthetic DAP^{2+} and, to some extent, the prokaryotic Put^{2+}) ability to disturb the DNA structure.

This and previous papers (Korolev et al. 2001, 2002, 2003, 2004) on the MD simulations of DNA in the compact environment and in the presence of polyamines reveal numerous differences between natural (Put^{2+}, Spd^{3+}, Spm^{4+}) and synthetic (DAP^{2+}) polyamines and gives some clues explaining the choice made by Nature between these similar compounds. Below we present a short account of the conclusions from this and previous work:

1. Polyamines, Na^+, and water interact most frequently with the charged O1P and O2P atoms. A preference to bind to the O1P atom of the phosphate (from the minor groove side) can be observed.
2. A rather short separation between the amino groups and a lower (than for Put^{2+}) hydrophobicity allows DAP^{2+} to find many electronegative "matches" on the surface of the DNA and leads to the formation of relatively stable DAP^{2+}–DNA complexes. This could also change local DNA hydration as well as the distribution of electropositive/electronegative sequence-dependent mosaics of the DNA molecule. A small fraction of divalent polyamines can be found in the major grooves, while spermidine or spermine are nearly absent in the major groove.
3. There is a strong anti-correlation of binding of polyamines to the sites of the DNA bases in the minor and in the major grooves: binding of an NH_3^+ group of polyamine or of Na^+ to one site practically excludes binding of another cation to the neighboring site situated less than 8 Å apart (Korolev et al. 2003).
4. The major difference between Spd^{3+} and all other cations studied in this work (DAP^{2+}, Put^{2+}, Na^+) is its weak binding in the major groove. Similarly, a very low presence of spermine in the major groove has been found in our previous work (Korolev et al. 2001, 2002). Spermine and spermidine are the most common eukaryotic polyamines and are present in the cell in millimolar amounts and concentrated in chromatin of the cell nucleus. The relatively low affinity of these polyamines to the sites in the major groove might be important in vivo since most regulatory proteins use a sequence-specific distribution of hydrogen bond donors and acceptors in the major groove for DNA reading and binding.
5. Most MD work uses Na^+ in studying the DNA solution and crystals. Sodium shows some specific

binding to sites in the DNA grooves, interacting strongly with the guanine O6 and N7 atoms in the major groove, and with the $T2_{O2}/T19_{O2}$ site in the minor groove.

Acknowledgements This work has been supported by the Swedish Science Research Council. N.K. acknowledges the support for a research fellowship from the School of Biological Sciences, NTU and from the Biomedical Research Council (BMRC), Singapore.

References

Allen MP, Tildesley DJ (1987) Computer simulations of liquids. Clarendon, Oxford

Bevan DR, Li L, Pedersen LG, Darden TA (2000) Molecular dynamics simulations of the $d(CCAACGTTGG)_2$ decamer: influence of the crystal environment. Biophys J 78:668–682

Bonvin AMJJ (2000) Localisation and dynamics of sodium counterions around DNA in solution from molecular dynamics simulations. Eur Biophys J 29:57–60

Chiu TK, Dickerson RE (2000) 1 Å crystal structures of B-DNA reveal sequence-specific binding and groove-specific bending of DNA by magnesium and calcium. J Mol Biol 301:915–945

Chiu TK, Kaczor-Grzeskowiak M, Dickerson RE (1999) Absence of minor groove monovalent cations in the crosslinked dodecamer C-G-C-G-A-*A*-T-T-C-G-C-G. J Mol Biol 292:589–608

Cohen SL (1998) A guide to the polyamines. Oxford University Press, New York

Drew HR, Dickerson RE (1981) Structure of a *B*-DNA dodecamer III. Geometry of hydration. J Mol Biol 151:535–556

Egli M (2002) DNA–cation interactions: quo vadis? Chem Biol 9:277–286

Hamelberg D, McFail-Isom L, Williams LD, Wilson WD (2000) Flexible structure of DNA: ion dependence of minor-groove structure and dynamics. J Am Chem Soc 122:10513–10520

Hamelberg D, Williams LD, Wilson WD (2001) Influence of the dynamic positions of cations on the structure of the DNA minor groove: sequence-dependent effects. J Am Chem Soc 123:7745–7755

Hamelberg D, Williams LD, Wilson WD (2002) Effect of a neutralized phosphate backbone on the minor groove of B-DNA: molecular dynamics simulation studies. Nucleic Acids Res 30:3515–3623

Ho SP, Mooers BHM (1997) Z-DNA crystallography. Biopolymers 44:65–90

Howerton SB, Sines CC, VanDerveer L, Williams LD (2001) Locating monovalent cations in the grooves of B-DNA. Biochemistry 40:10023–10031

Hud NV, Schultze P, Sklenár V, Feigon J (1999) Binding sites and dynamics of ammonium ions in the minor groove of DNA duplexes in solution and the origin of DNA A-tract bending. J Mol Biol 286:651–660

Igarashi K, Kashiwagi K (2000) Polyamines: mysterious modulators of cellular functions. Biochem Biophys Res Commun 271:559–564

Korolev N, Lyubartsev AP, Nordenskiöld L, Laaksonen A (2001) Spermine: an ''invisible'' component in the crystals of *B*-DNA. A grand canonical Monte Carlo and molecular dynamics simulation study. J Mol Biol 308:907–917

Korolev N, Lyubartsev AP, Laaksonen A, Nordenskiöld L (2002) On the competition between water, sodium ions, and spermine in binding to DNA. A molecular dynamics computer simulation study. Biophys J 82:2860–2875

Korolev N, Lyubartsev AP, Laaksonen A, Nordenskiöld L (2003) A molecular dynamics simulation study of oriented DNA with polyamine and sodium counterions: diffusion and averaged binding of water and cations. Nucleic Acids Res 30:5971–5981

Korolev N, Lyubartsev AP, Laaksonen A, Nordenskiöld L (2004) Molecular dynamics simulation study of oriented polyamine– and Na–DNA: sequence specific interactions and effects on DNA structure. Biopolymers 73:542–555

Kosikov KM, Gorin AA, Lu X-J, Olson WK, Manning GS (2002) Bending of DNA by asymmetric charge neutralization: all-atom energy simulations. J Am Chem Soc 124:4838–4847

Lindsay SM, Lee SA, Powel JW, Weidlich T, DeMarco C, Lewen GD, Tao NJ, Rupprecht A (1988) The origin of the A to B transition in DNA fibers and films. Biopolymers 27:1015–1043

Lohikoski RA, Timonen J, Lyubartsev AP, Laaksonen A (2003) Internal structure and dynamics of the decamer $d(ATG-CAGTCAG)_2$ in Li^+-H_2O solution. A molecular dynamics simulation study. Mol Simul 29:47–62

Luger K, Richmond TJ (1998) DNA binding within the nucleosome core. Curr Opin Struct Biol 8:33–40

Luger K, Mader AW, Richmond RK, Sargent DF, Richmond TJ (1997) Crystal structure of the nucleosome core particle at 2.8 Å resolution. Nature 389:251–260

Lyubartsev AP, Laaksonen A (1998) Molecular dynamics simulations of DNA in solution with different counter-ions. J Biomol Struct Dyn 16:579–592

Lyubartsev AP, Laaksonen A (2000) M.Dyna *Mix* - a scalable portable parallel MD simulation package for arbitrary molecular mixtures. Comput Phys Commun 128:565–589

MacKerell AD, Wiorkiewiczkuczera J, Karplus M (1995) An all-atom empirical energy function for the simulation of nucleic-acids. J Am Chem Soc 117:11946–11975

Maher JL (1998) Mechanisms of DNA bending. Curr Opin Chem Biol 2:688–694

Manning GS, Ebralidze KK, Mirzabekov AD, Rich A (1989) An estimate of the extent of folding of nucleosomal DNA by laterally asymmetric neutralization of phosphate groups. J Biomol Struct Dyn 6:877–889

Martyna GJ, Tobias DJ, Klein ML (1994) Constant pressure molecular dynamics algorithms. J Chem Phys 101:4177–4189

McConnell KJ, Beveridge DL (2000) DNA structure: what's in charge? J Mol Biol 304:803–820

McFail-Isom L, Sines CC, Williams LD (1999) DNA structure: cations in charge? Curr Opin Struct Biol 9:298–304

Shui X, Sines CC, McFail-Isom L, VanDerveer L, Williams LD (1998) Structure of the potassium form of CGCGAATTCGCG: DNA deformation by electrostatic collapse around inorganic cations. Biochemistry 37:16877–16887

Sines CC, McFail-Isom L, Howerton SB, VanDerveer L, Williams LD (2000) Cations mediate B-DNA conformational heterogeneity. J Am Chem Soc 122:11048–11056

Smith DE, Dang LX (1994) Computer-simulations of NaCl association in polarizable water. J Chem Phys 100:3757–3766

Song Z, Antzutkin ON, Lee YK, Shekar SC, Rupprecht A, Levitt MH (1997) Conformational transitions of the phosphodiester backbone in native DNA: two-dimensional magic-angle spinning ^{31}P-NMR of DNA fibers. Biophys J 73:1539–1552

Stofer E, Lavery R (1994) Measuring the geometry of DNA grooves. Biopolymers 34:337–346

Thomas T, Thomas TJ (2001) Polyamines in cell growth and cell death: molecular mechanisms and therapeutic applications. Cell Mol Life Sci 58:244–258

Timsit Y, Moras D (1992) Crystallization of DNA. Methods Enzymol 211:409–429

Toukan K, Rahman A (1985) Molecular-dynamics study of atomic motions in water. Phys Rev B 31:2643–2648

Tuckerman M, Berne B, Martyna GJ (1992) Reversible multiple time scale molecular-dynamics. J Chem Phys 97:1990–2001

van Dam L, Korolev N, Nordenskiöld L (2002) Polyamine mobility and effect on DNA structure in oriented DNA fibers. Nucleic Acids Res 30:419–428

Williams LD, Maher JL (2000) Electrostatic mechanisms of DNA deformation. Annu Rev Biophys Biomol Struct 29:497–521

York DM, Yang W, Lee H, Darden T, Pedersen LG (1995) Toward the accurate modeling of DNA: the importance of long-range electrostatics. J Am Chem Soc 117:5001–5002